[1]Yongsheng Zhao
[1]Nan Zhang
[2]Bin Wu
[3]Jian Zhang
[1]Ming Zhao
[1]Junhao Xiao

Fault-tolerant Integration of Charge and Discharge Information Security for Multi-Scale Time Series Models

Journal of Electrical Systems

Abstract: - In this paper, the power mode of winding and converter topology are integrated. Considering the filter characteristics and electromagnetic torque control of the system during charging/discharging, the integrated structures of one-phase full bridge, three-phase full bridge and three-phase four-arm bridge are studied. The single-phase all-bridge integrated structure can completely suppress the electromagnetic torque generated by the motor during charging and discharging, and make the filtering effect of the system better. In this project, a multi-scale full convolutional deep neural network method based on time series is studied. The multi-scale full convolution time series model is used for training, and the future continuous signals can be monitored according to the trained model based on the power signal data collected from high-voltage power lines. Experiments show that the proposed method can effectively extract the required data.

Keywords: High-Voltage Transmission; Long Short-Term Memory Network; Multi-Scale; Full Convolution; Deep learning; Partial Discharge.

I. INTRODUCTION

Aiming at the problem of charging/discharging of electric vehicles, a charging/discharging system based on on-board battery was proposed. For a car, however, charging and discharging devices on the car will make the body bigger and heavier; At the same time, due to the development of power electronic equipment and the continuous progress of control means, higher requirements are put forward for high power density controllers. Therefore, miniaturization, lightweight, low cost, high integration and high power density controller is the future development direction [1].

In the field of engineering, the charging and discharging information security fault-tolerant integration method of multi-scale timing models is a technology used to improve the reliability and safety of power systems or energy storage systems during the charging and discharging process. This method usually involves the following key steps:

1. Modeling and Prediction: First, the behavior of the energy storage system needs to be modeled, which may involve multiple levels from the micro scale to the macro scale. The microscale may focus on the charge and discharge behavior of a single battery or battery module, while the macroscale may focus on the performance of the entire energy storage system.

2. Data collection and processing: Collect data generated during the charging and discharging process in real time. After processing, these data can be used to train and verify multi-scale time series models.

3. Fault-tolerant mechanism design: In order to ensure that the system remains stable and safe when a fault occurs or operates abnormally, a corresponding fault-tolerant mechanism needs to be designed. This may include setting thresholds, implementing dynamic adjustment of charge and discharge strategies, and using redundant designs to improve system robustness.

4. Security Assessment and Optimization: Use the established model to conduct security assessment, identify potential security risks, and propose optimization measures for these risks. This may involve sensitivity analysis of the model, quantitative risk assessment, etc.

5. Integration and Implementation: Combine the above steps to form a complete integration solution. This includes integrating the model into the actual control system to achieve real-time monitoring and automatic adjustment to cope with various possible charging and discharging scenarios.

[1] State Grid Information & Telecommunication Group Co., Ltd. Beijing 102211, China
[2]GRID Corporation of China, Beijing 102211, China
[3]State Grid Tianjin Electric Power Company, Tianjin, 300143, China
*Corresponding author e-mail: Nan Zhang

Through this multi-scale timing model charging and discharging information security and fault-tolerant integration method, the performance, safety and reliability of the energy storage system can be significantly improved, while reducing maintenance costs and extending system life. When designing and implementing such a system, multiple uncertainties and changing factors in the actual operating environment also need to be taken into account to ensure that the system can perform well under various circumstances. At present, there are two different control methods of automobile charging and motor transmission, which realize the organic combination of the two. In recent years, researchers at home and abroad have begun to pay attention to a new generation of energy storage systems, and for various situations, given the circuit structure suitable for various situations. In highly integrated power electronic equipment, because the alternating current flowing through the coil will produce electromagnetic torque in the motor, how to effectively suppress or suppress electromagnetic torque has become the focus of research [2]. Stator winding power mode and motor winding design and optimization.

Some researchers have proposed to integrate the three-phase full bridge drive and charging, and transform it into a BoostPFC structure, that is, the asynchronous motor coil is used as a filter coil, and the switch between the two ways is completed through the relay to meet the needs of single-phase small electric vehicles [3]. Some scholars suggest using a novel four-way switching converter to drive electric vehicles. Compared with six-way switching, the number of converters required is relatively less, but diode rectification is required in the subsequent stage, and zero sequence current affects the operating efficiency of the entire system [4]. At present, studies have shown that the multi-inverter power system is a new type of multi-converter compound multi-inverter power system, which is led from the Central Line of multiple motors through the midpoint position of multiple motors, so that the operation of multiple motors and single-phase charging are highly integrated, and its structure is expensive, only suitable for four-wheel drive vehicles. For the first time, researchers have proposed a new type of Z-source converter, which only uses the rear two-phase winding to form a single-phase charger, and the first-phase winding is in an open state, and the induction coefficient utilization is not high [5]. This project plans to use the method of two phases in parallel and another phase winding for power supply, but the motion of the motor when charged is not considered. Some scholars believe that under the charging mode, the stator coil of the motor and the inverter form a three-phase staggered parallel Boost loop, because the same current flows through the three stators, so there is no electromagnetic field torque, but its disadvantage is that only through the one-way current, must be installed additional filtering device to suppress the harmonic current.

Existing studies start from the structure of the motor coil and study the method introduced by it, that is, the intermediate point tap is used to make the two coils pass the balanced current, thus overcoming the problem of rotor rotation [6]. However, due to the addition of double switching devices, the difficulties and costs of manufacturing and manufacturing are greatly increased, and there is a large number of mutual coupling between the coils. Making it difficult to achieve a balanced current balance. Chalmers University of Technology in Sweden proposed a new two-stator structure charging module for the first time based on the research of motor coil configuration. A high-power, high-power, high-efficiency non-insulated, non-insulated, non-insulated three-phase charging device based on embedded PMSM was designed. These two architectures lead to the complexity of the system, the difficulty of design and manufacture, and the difficulty of control [7]. The common problems in the existing research are as follows: the composition of the driver is relatively complex, and there are more switching components; After the transformation of the motor coil, its structure becomes more complicated, the manufacturing is difficult, and the cost increases accordingly. Under charging and discharging conditions, additional mechanisms must be added due to the existence of torque inside the motor. A new method of brushless DC motor based on rotor rotation is presented[8].

Explore an integrated power/energy storage topology for electric vehicles from the vantage point of an open electric vehicle motor; Aiming at the problem of low electromagnetic torque in charging and discharging stage of electric vehicle, the integrated electric storage topology is studied. The electrical characteristics of single-phase full-bridge converter, three-phase full-bridge converter and three-phase four-leg converter are compared. In addition, the challenge of electromagnetic torque under different excitation modes is studied through the lens of stator windings in series.

II. INTEGRATED TOPOLOGY OF MOTOR DRIVE AND CHARGE AND DISCHARGE

An electric motor and a corresponding control system. The traditional automobile motor drive system is shown in Figure 1 (the picture is quoted in Advanced power inverter topologies and modulation techniques for common-mode voltage elimination in the picture) electric motor drive systems). The onboard charge and discharge system is shown in Figure 2 (image cited in Electronics 2020, 9(10), 1738). The device consists of

battery, DC-DC converter, single/three-phase full bridge converter, filter, power grid and control [9]. The two control parts work separately. When the vehicle is running, the motor drives the whole system. When the vehicle stops running, the battery is charged and discharged, and the motor transmission conversion device is idle at this time. At the same time, the motor and the car charging device adopt the same architecture, so the electric vehicle can be recombined under the two ways of charging and discharging to form the car charging and discharging device. In addition, the method can also transform the motor winding into a capacitive capacitor on the grid side to reduce or remove excess capacitance. The IC architecture has many functions such as motor drive, rectifier charging and inverter access, and the integration is greatly improved compared with the conventional independent system.

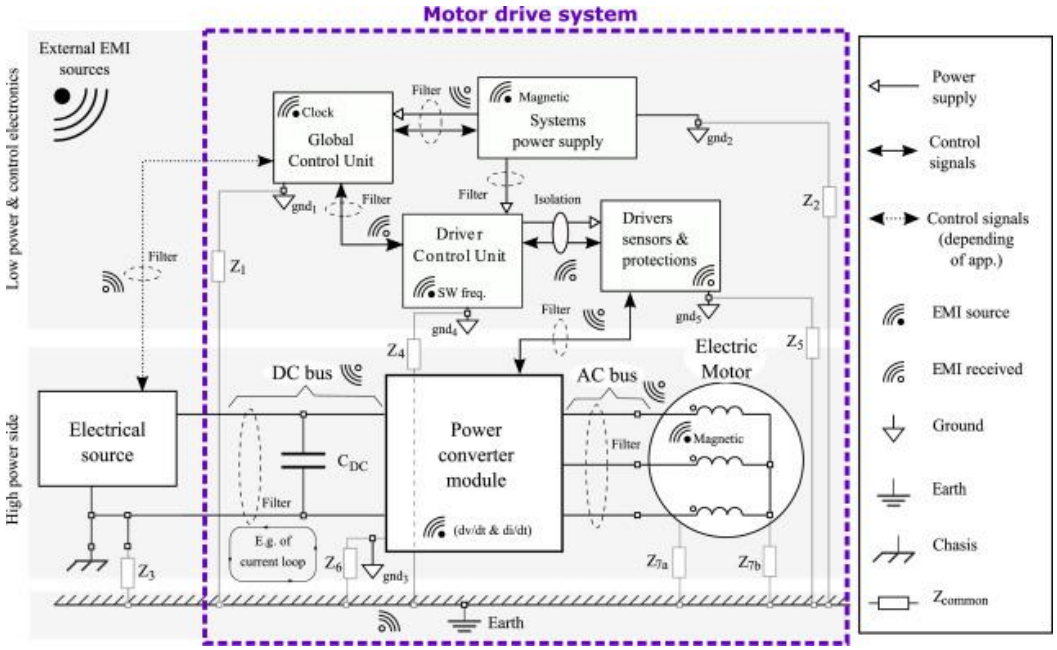

Fig.1 Topology of motor drive system

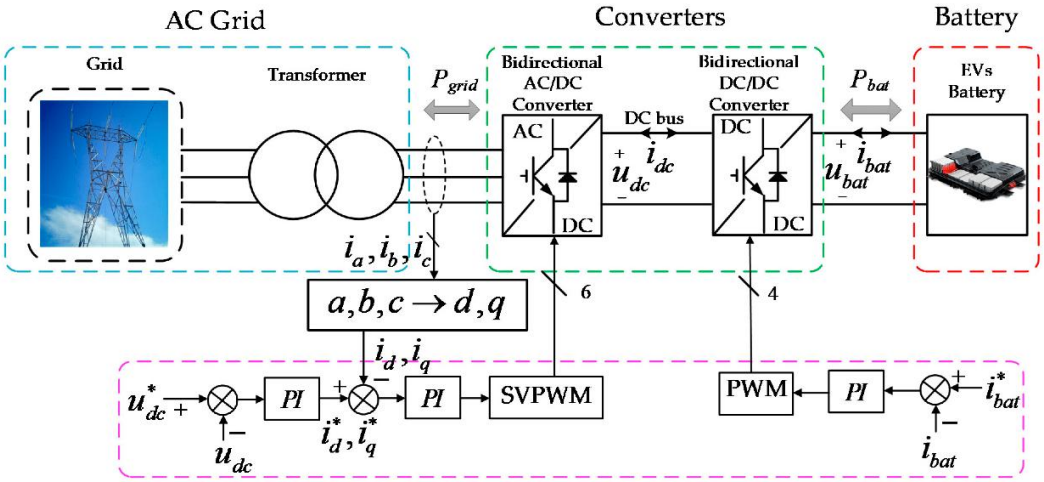

Fig.2 Topology of charge and discharge system

In the state of charging and discharging, the motor winding is opened and connected to the power grid through switching components to form a bidirectional flow of energy storage and electric energy. At the same time, the stator coil of the motor is constructed as a network filter to filter the current entering the network, so as to reduce the voltage distortion of the network during charging and discharging [10]. If there is alternating current flowing through the coil, it will cause motor rotation or vibration, affecting the smooth operation of the motor, but also cause rotation loss. Therefore, from the Angle of reducing torque, the transmission structure and winding of the motor are reformed. Figure 3 shows an integrated system of motor drive and charge and discharge (image cited in DC Microgrid Integrated Electric Vehicle Charging Station Scheduling Optimization).

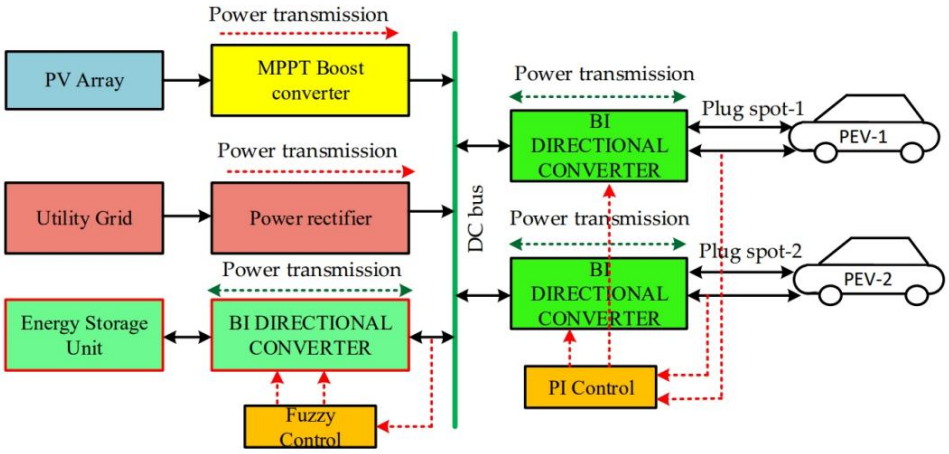

Fig.3 Topology of integrated system of motor drive and charge and discharge

The configuration of fixed rotor winding is studied from the motor body in order to achieve the optimal integration. This project intends to combine the above two research ideas innovatively for the existing vehicle type energy storage device, that is, to realize the integrated optimization of the drive circuit, and to consider the overall design of the motor; It is also necessary to avoid the control difficulty and increase the cost caused by the design of the coil. Therefore, the integrated topology of the vehicle type energy storage battery is realized based on ensuring no control complexity caused by the design of the motor coil and increasing its cost [11]. According to the different transmission structure, it is divided into single-phase full-bridge transformation mode, three-phase full-bridge transformation mode and three-phase four-arm transformation mode, respectively from the electromagnetic torque, system structure, motor complexity, filtering performance and other aspects of the comparison.

A. Single-phase full-bridge conversion Mode

The comprehensive topology of single-phase full-bridge conversion is shown in Figure 4 (image cited in Electronics 2018, 7(5), 62), where the single-phase full-bridge conversion circuit is composed of the front two bridge arms in charging and discharging mode. In the case of single-phase charging and discharging, the motor windings are divided into five types in order to reduce the filter inductance and give full play to the motor's sensibility. The invention relates to a two-phase parallel stator coil and a three-phase winding.

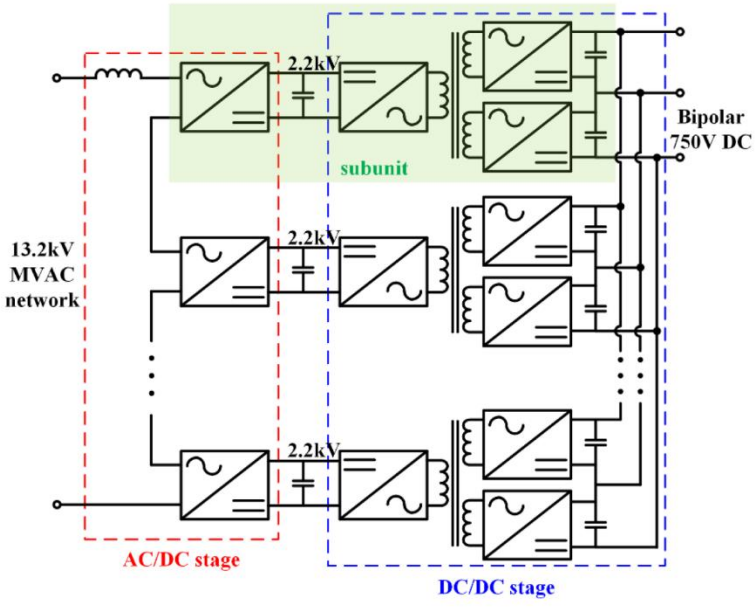

(a)

Fig.4 Overall structure of single-phase full-bridge conversion

B. Three-phase full-bridge conversion mode

The comprehensive topology of the three-phase full-bridge conversion is shown in Figure 5 (image cited in Solar Hybrid Systems for Smart Grids). The three-phase full bridge charging and discharging mode is used for charging and discharging [12]. The three-phase stator coil of the motor can be reorganized according to the wiring mode shown in Figure 5, and its construction number is VI: the two-phase coil is parallel to the other one-phase coil, that is, the A coil and the B coil are in parallel, and then the C phase is connected in series. By controlling the same switching signal for A given VT1 and VT3, the same current flows through phases A and B.

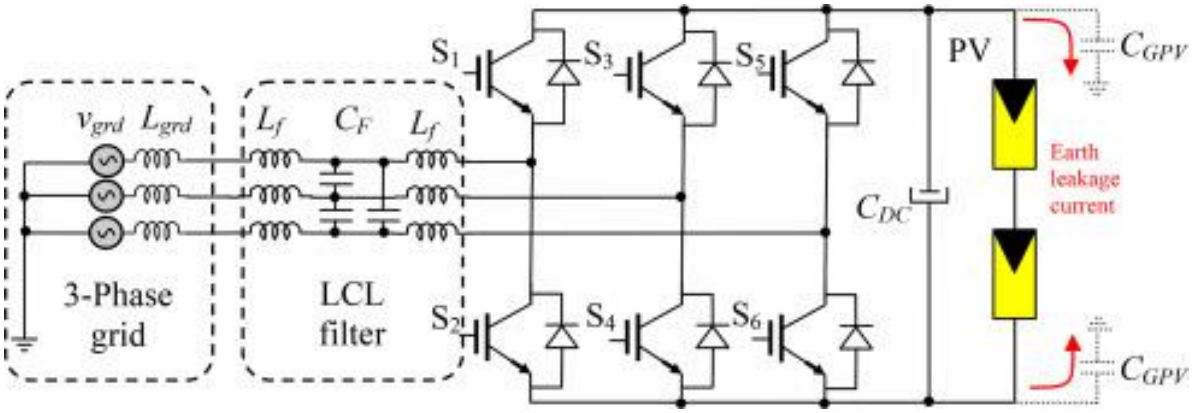

Fig.5 Overall structure of three-phase full-bridge conversion

III. THREE-PHASE FOUR-ARM BRIDGE CONVERSION MODEL

A bridge arm was added to the three-phase full bridge in the first stage to form a three-phase bridge arm with four arms. For the single-phase rechargeable battery, the three-phase stator windings of the motor are reconstructed into the wiring form as shown in Figure 6, that is, the three-phase stator windings of A, B and C are connected to the power grid by the lead wire at the middle point, so that the three-phase stator windings of A, B and C flow equal current through the control [13]. Figure 6 shows that under the single-phase full-bridge drive charging mode, when the coil connection form is IV structure, Motor speed and electromagnetic torque waveform (picture cited in The Case Study of Simulation of Power Converter Circuits Using Psim Software in Teaching). The series winding connection structure II, III and V will also have a similar situation, which is not conducive to the smooth operation of the system.

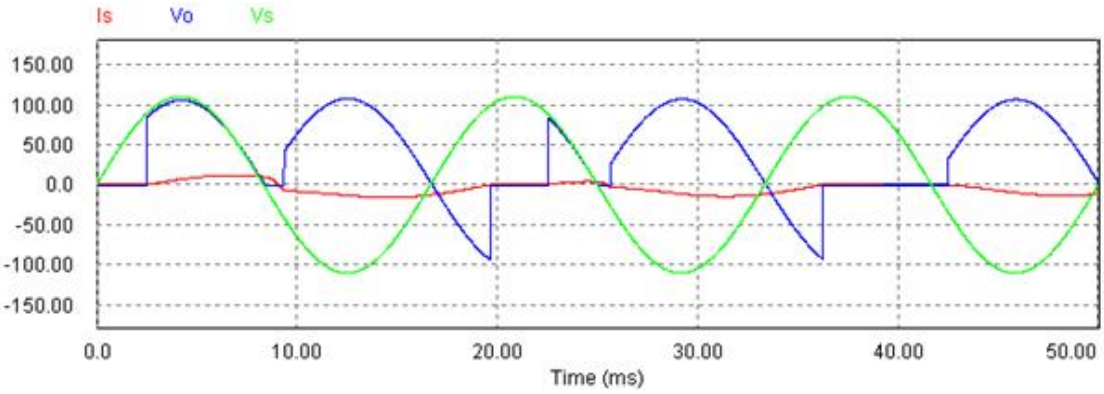

Fig.6 Simulation waveform of speed and torque in single-phase full-bridge conversion mode

By comparing the three different driving modes, it can be seen that the three different driving modes have strong electromagnetic torque suppression performance, and can effectively solve the rotor rotation problem caused by the inflow of AC current in the charging process [14]. However, considering the filter performance, motor winding structure and the number of switching devices and other factors, under the single-phase full-bridge conversion mode, When each phase winding is arranged as III-V, its performance will be superior. In order to simulate the characteristic index of single-phase full-bridge conversion mode, this project intends to combine the side coil of the network and the motor coil in series to form a filter, and study that single-phase full-bridge conversion can achieve unit power factor operation under both charging/discharging conditions, and the

network current and network voltage are at the same frequency, and the current follows the voltage, and the PR controller is adjusted without static difference. The actual current is stabilized at 15 A, and after Fourier transform, the current THD=2.64% is obtained, and THD=2.90% is not inserted into the motor coil. The experimental results show that the design scheme is feasible. It conforms to the national standard THD<5%.

IV. DATABASE AND LSTM

A. Data Set

The experimental data studied are extracted from the high voltage power spectrum data published on the Internet, and some of the samples contain the photocurrent in the process of photodischarge. The voltage measuring device is placed on the three-phase high-voltage power line of 50 Hz to collect the 3-phase voltage signal. In this system, it works for 20 milliseconds [15]. The meter takes just 20 milliseconds to collect 800,000 samples in one cycle. The single sampling point used in this paper is the high-voltage power signal measured during one-phase operation. All sampled voltage signals in the data set are scaled down to [-128,127] and rounded to integers. FIG. 7 shows the sample without partial discharge phenomenon and the sample with partial discharge phenomenon (the picture is quoted in Energies 2021, 14(24), 8579).

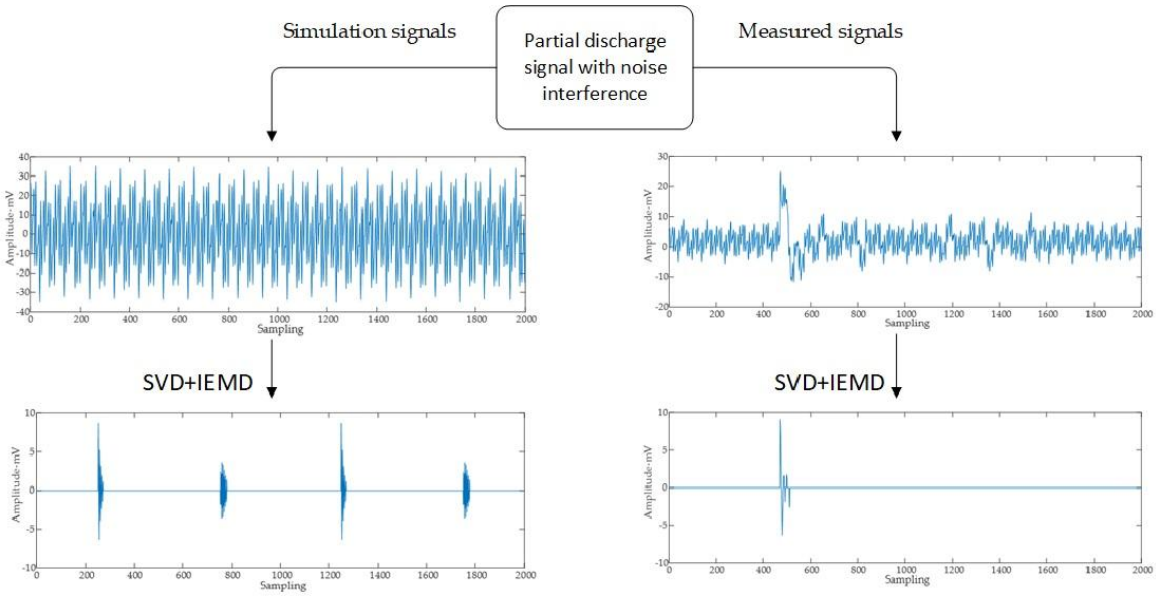

Fig.7 Samples without and with partial discharge phenomena

B. LSTM

For time series data, conventional neural networks show great limitations in this respect. Conventional artificial neural networks have difficulty distinguishing between different events at different time periods and cannot infer subsequent events based on events that have already occurred in the film. However, this problem can be overcome by using ring neural network. Because the loop neural network has the ability of extracting time sequence information and retaining information [16]. The module B of the neural network reads a certain input u_t and outputs a value g_t after processing. And each module will pass the processed message to the next module, so that this network structure can retain some timing information.

$$y_t^h = \delta(\eta^h g_{t-1} + E^h u_t) \tag{1}$$

Where η^h, E^h represents the weight of g_{t-1} and u_t respectively. The value of y_t^h ranges from 0 to 1. 1 indicates that the value is retained completely, and 0 indicates that the value is discarded completely [17]. The function of the input gate is to filter the information of the input u_t, which is represented here by y_t^i.

$$y_t^v = \delta(\eta^v g_{t-1} + E^v u_t) \tag{2}$$

$$y_t^z = \tanh(\eta^z g_{t-1} + E^z u_t) \tag{3}$$

$$y_t^i = y_t^v \odot y_t^z \tag{4}$$

Where η^v, η^z represents the weight of g_{t-1} and E^v, E^z represents the weight of u_t. The role of the output gate determines the content of the current state output, which is represented here by g_t. It is mainly affected by y_t^o, and the resulting Z_t is reduced by tanh activation function. The three formulas are as follows:

$$y_t^o = \delta(\eta^o g_{t-1} + E^o u_t) \tag{5}$$

$$Z_t = y_t^h \odot Z_{t-1} + y_t^i \tag{6}$$

$$g_t = tanh(y_t^o \odot Z_t) \tag{7}$$

Where η^o, E^o represents the weight of g_{t-1} and u_t respectively. The short - and long-term memory model in LSTM-MCNN requires spatial transformation. The LSTM layer of the LSTM block is also set to 128 cells. Finally, set Dropout to 0.8.

V. EXPERIMENT

A. Experimental design

This project intends to divide high-voltage time series signals into 5 groups through 5 interactive testing methods, among which 1 group is the test group and 4 group is the training group [18]. As the local discharge problem of high voltage time series belongs to the second class problem, this project learns the model at the cost of binary cross approximation.

$$loss = -y \ln(\tilde{y}) - (1-y)\ln(1-\tilde{y}) \tag{8}$$

Where $y \in \{0,1\}$ represents the real label of the sample, and $\tilde{y} \in \{0,1\}$ represents the predicted value of the model for the sample. Each function is executed 100 times, and the batch-size is 128. This project intends to adopt a variety of deep neural network models such as LSTM, LSTM-FCN, and bidirectional LSTM based on attention mechanism, and verify the effectiveness of the developed deep learning algorithm by comparing with various existing deep neural network recognition algorithms. The number of cells in the LSTM section is set to 128 in each mode.

B. Evaluation criteria

Because the experiment I was engaged in was a category two problem. Since the data used were very uneven, Matthews' correlation was selected for evaluation. In essence, MCC is a correlation factor used to describe the real category and the forecast category. Measures that measure unbalanced data sets are better. MCC is calculated as follows:

$$M_{MCC} = \frac{T_P T_N - F_P F_N}{\sqrt{(T_P + F_P)(T_P + F_N)(T_N + F_P)(T_N + F_N)}} \tag{9}$$

C. Experimental Results

Figure 8 shows how the values of MCC and loss corresponding to the training set and the confirmation set change with the increase of iterations during the training period in the five interactive tests [19]. The results show that the other three algorithms have good convergence except LSTM, among which LSTM-MCNN proposed by the author has the best convergence. Because the high-voltage signal used is a very unbalanced set of positive and negative samples, it is also subject to minor changes in the model when learning.

Table 1 shows the performance of the high-voltage time series signal data set under four modes, expressed as MCC values, with red symbols representing the best results. The LSTM-MCNN method introduced by the author is the most effective. And faster, too. It can be seen from the ROC curve that the LSTM-MCNN designed by the author is the best for PD detection.

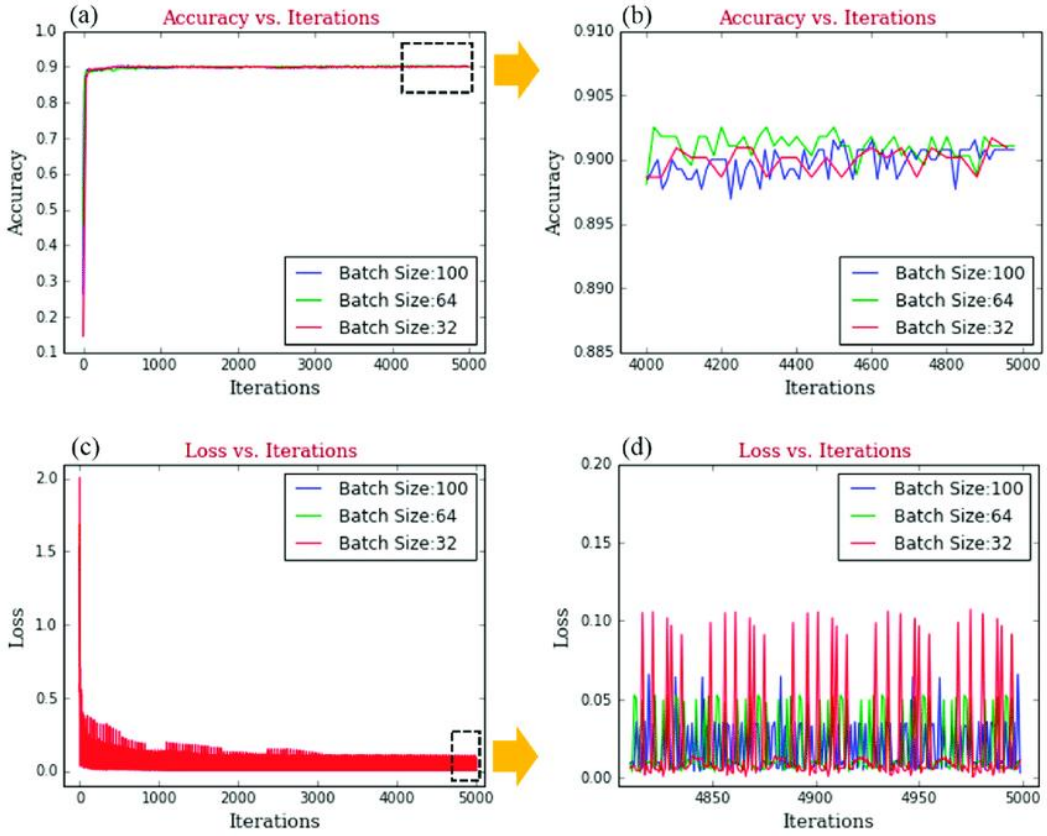

Fig.8 MCC and loss change curve with training

Table 1 MCC values of the four methods in the high-voltage power timing signal dataset

model	MCC	Seconds per epoch
LSTM	0.682	5
LSTM-FCN	0.783	5
BDLSTM	0.774	16
LSTM-MCNN	0.810	5

The LSTM-MCNN model studied in this project has the best performance for PD diagnosis. It provides an efficient and accurate deep learning algorithm for PD diagnosis. This project intends to adopt a single-phase full-bridge structure, only two bridge arms at the first end are used in the charging/discharging process, and charge and discharge tests are conducted on them to verify the proposed theoretical model. The system uses STM32F103 as the control core of the system to complete the communication on the input side [20]. The voltage sensor samples the grid voltage and the DC bus voltage, while the current sensor samples the voltage on the grid side, and sends it to the ARM controller through the appropriate regulation circuit for calculation and generates the corresponding switching signal. The generated pulse-width modulation switching signal activates the corresponding switching tube, so that the switching tube VT1 and VT2 are complementary on, and VT3 and VT4 are complementary on. The PMSM has an output current of 50 Hz, an RMS of 220 V, a switching frequency of 15 kHz, an inductance of 2 mH, an inductance of 0.15 mH per phase winding, a Udc at the DC end, and a DC-end filter of 4500 μF. The hardware block diagram is shown in Figure 9 (the image is referenced to the Battery Management System Subsystems and Their Influence).

The single phase full bridge drive is adopted to make it have better comprehensive efficiency. Taking the structure of type IV winding as the object, the equivalent winding structures of II, III and V are designed, and the steady-state charging test is carried out to compare and compare the operating characteristics of each winding before and after parallel connection. FIG. 10 shows the test results of 2 mH on the grid side when there is no series motor inductance value in the single-phase full-bridge conversion circuit. In the case that there is no series coil and only the grid coil is used as the filter, 400 V power supply is applied to the outer loop of the voltage. Compared with the measured DC bus voltage Udc=406 V, the deviation is about 1%, which is within the acceptable limit. The action value of ig at the end of the network is 12.9A, which can make the system achieve

the purpose of no static error. The circuit has the same frequency as the grid, 180 degrees of phase difference, with 9.87A actual current and 9.90A current closed loop, confirming that the use of PR controller can achieve the purpose of no static difference adjustment. The experimental results show that the application of single-phase full-bridge circuit in charging and discharging is feasible.

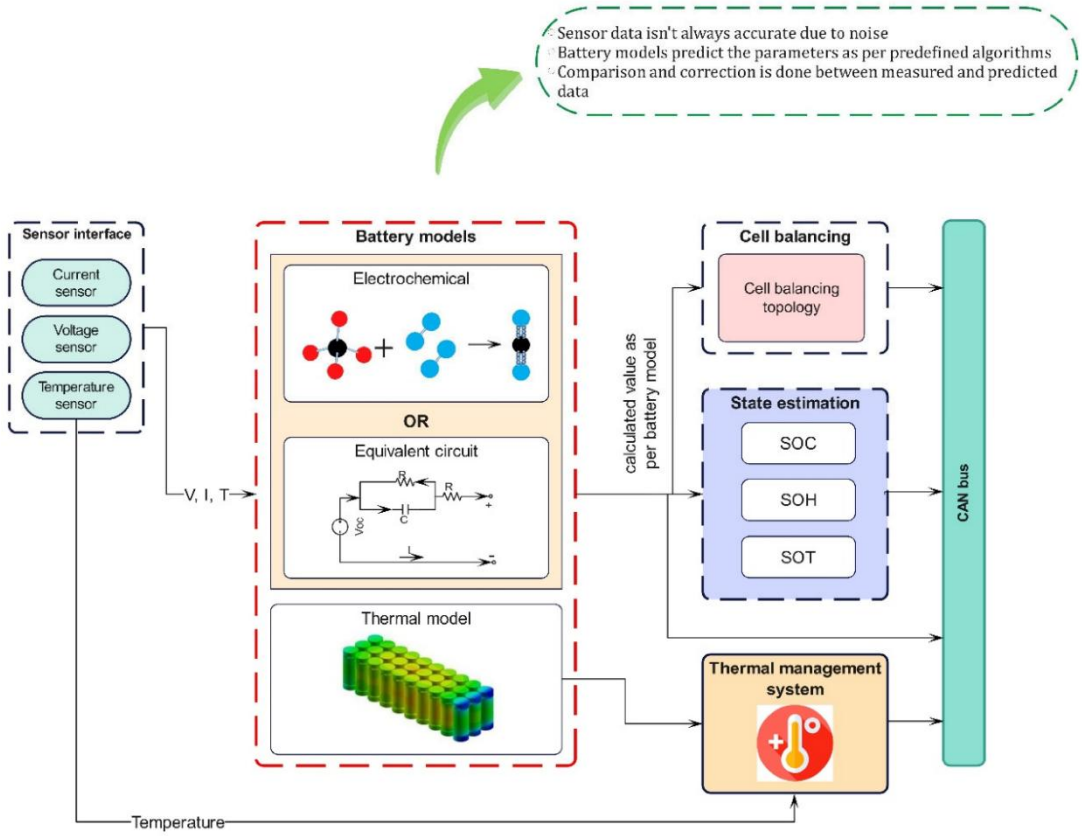

Fig.9 Hardware block diagram of integrated charge and discharge system based on open circuit of motor winding

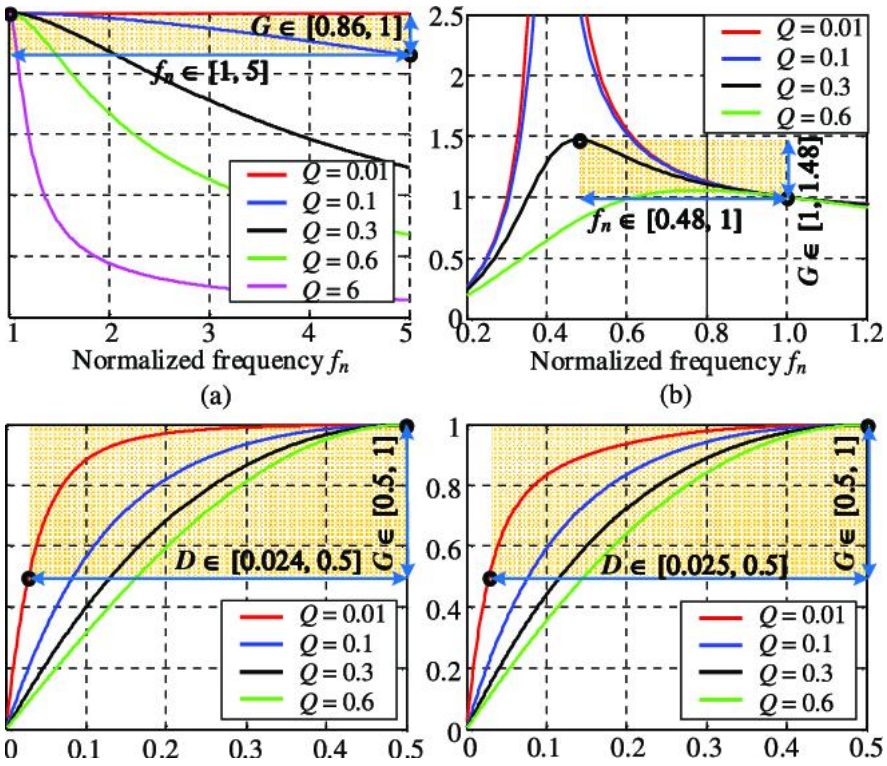

Fig.10 Single phase full bridge conversion mode is not seriated into the motor winding

VI. CONCLUSION

In order to find the fault as early as possible, timely maintenance and repair, reduce unnecessary economic losses, plays a very important role in the safe operation of the power grid. However, due to time dependence, conventional machine learning methods and deep convolutional neural networks cannot accurately extract time-dependent features, thus reducing the accuracy of prediction. Therefore, this project intends to apply short term memory method in deep neural network to PD detection, and construct multi-scale full convolutional neural network and LSTM joint modeling method. A fault diagnosis method based on time series is proposed. It is proved by experiments that the detection technique described in this paper can detect the situation of serious non-uniformity of positive and negative samples.

ACKNOWLEDGEMENTS

State Grid Tianjin Electric Power Company" Research and demonstration of key technologies for low-voltage DC charging and discharging systems for electric vehicles in residential communities" (No.:5400-202312239A-1-1-ZN).

REFERENCES

[1] Garcia-Torres, F., Bordons, C., Tobajas, J., Márquez, J. J., Garrido-Zafra, J., & Moreno-Muñoz, A. (2020). Optimal schedule for networked microgrids under deregulated power market environment using model predictive control. IEEE Transactions on Smart Grid, 12(1), 182-191.

[2] Yu, Q., Wan, C., Li, J., Xiong, R., & Chen, Z. (2021). A model-based sensor fault diagnosis scheme for batteries in electric vehicles. Energies, 14(4), 829.

[3] Ding, R., Cheng, M., Jiang, L., & Hu, G. (2020). Active fault-tolerant control for electro-hydraulic systems with an independent metering valve against valve faults. IEEE Transactions on Industrial Electronics, 68(8), 7221-7232.

[4] Yan, C., Chen, J., Liu, H., Kumar, L., & Lu, H. (2020). Health management for PEM fuel cells based on an active fault tolerant control strategy. IEEE Transactions on Sustainable Energy, 12(2), 1311-1320.

[5] Xu, L., Ma, R., Xie, R., Xu, J., Huangfu, Y., & Gao, F. (2021). Open-circuit switch fault diagnosis and fault-tolerant control for output-series interleaved boost DC–DC converter. IEEE Transactions on Transportation Electrification, 7(4), 2054-2066.

[6] Sharma, V., Gupta, N., Shah, A. P., Vishvakarma, S. K., & Chouhan, S. S. (2021). A reliable, multi-bit error tolerant 11T SRAM memory design for wireless sensor nodes. Analog Integrated Circuits and Signal Processing, 107(2), 339-352.

[7] Tao, Y., Qiu, J., & Lai, S. (2021). A hybrid cloud and edge control strategy for demand responses using deep reinforcement learning and transfer learning. IEEE Transactions on Cloud Computing, 10(1), 56-71.

[8] Zhang, K., Hu, X., Liu, Y., Lin, X., & Liu, W. (2021). Multi-fault detection and isolation for lithium-ion battery systems. IEEE Transactions on Power Electronics, 37(1), 971-989.

[9] Liu, P., Wang, C., Hu, J., Fu, T., Cheng, N., Zhang, N., & Shen, X. (2020). Joint route selection and charging discharging scheduling of EVs in V2G energy network. IEEE Transactions on Vehicular Technology, 69(10), 10630-10641.

[10] Jiang, J., Chen, J., Li, J., Yang, X., Bie, Y., Ranjan, P., ... & Schwarz, H. (2021). Partial discharge detection and diagnosis of transformer bushing based on UHF method. IEEE Sensors Journal, 21(15), 16798-16806.

[11] Han, W., Wik, T., Kersten, A., Dong, G., & Zou, C. (2020). Next-generation battery management systems: Dynamic reconfiguration. IEEE Industrial Electronics Magazine, 14(4), 20-31.

[12] Guo, J., Liu, S., Zhu, L., & Lombardi, F. (2020). Design and evaluation of low-complexity radiation hardened CMOS latch for double-node upset tolerance. IEEE Transactions on Circuits and Systems I: Regular Papers, 67(6), 1925-1935.

[13] Wen, H., Li, J., Shi, H., Hu, Y., & Yang, Y. (2020). Fault diagnosis and tolerant control of dual-active-bridge converter with triple-phase shift control for bidirectional EV charging systems. IEEE Transactions on Transportation Electrification, 7(1), 287-303.

[14] Sharma, V., Gupta, N., Shah, A. P., Vishvakarma, S. K., & Chouhan, S. S. (2021). A reliable, multi-bit error tolerant 11T SRAM memory design for wireless sensor nodes. Analog Integrated Circuits and Signal Processing, 107(2), 339-352.

[15] Lashab, A., Yaqoob, M., Terriche, Y., Vasquez, J. C., & Guerrero, J. M. (2020). Space microgrids: New concepts on electric power systems for satellites. IEEE Electrification Magazine, 8(4), 8-19.

[16] Nimalsiri, N. I., Ratnam, E. L., Smith, D. B., Mediwaththe, C. P., & Halgamuge, S. K. (2021). Coordinated charge and discharge scheduling of electric vehicles for load curve shaping. IEEE Transactions on Intelligent Transportation Systems, 23(7), 7653-7665.

[17] Lv, C., Chang, J., Bao, W., & Yu, D. (2022). Recent research progress on airbreathing aero-engine control algorithm. Propulsion and Power Research, 11(1), 1-57.

[18] Lin, T., Chen, Z., Zheng, C., Huang, D., & Zhou, S. (2020). Fault diagnosis of lithium-ion battery pack based on hybrid system and dual extended Kalman filter algorithm. IEEE transactions on transportation electrification, 7(1), 26-36.

[19] Stojanovic, V., & Prsic, D. (2020). Robust identification for fault detection in the presence of non-Gaussian noises: application to hydraulic servo drives. Nonlinear Dynamics, 100(3), 2299-2313.

[20] Schmid, M., Gebauer, E., Hanzl, C., & Endisch, C. (2020). Active model-based fault diagnosis in reconfigurable battery systems. IEEE Transactions on Power Electronics, 36(3), 2584-2597.